Chemical Science

ROYAL SOCIETY OF CHEMISTRY

EDGE ARTICLE

View Article Online
View Journal | View Issue

Cite this: *Chem. Sci.*, 2020, **11**, 10127

All publication charges for this article have been paid for by the Royal Society of Chemistry

Received 18th June 2020
Accepted 28th August 2020

DOI: 10.1039/d0sc03391j

rsc.li/chemical-science

A rationally designed peptoid for the selective chelation of Zn^{2+} over Cu^{2+}†

Pritam Ghosh and Galia Maayan *

The selective removal of Zn^{2+} from proteins by using a synthetic chelator is a promising therapeutic approach for the treatment of various diseases including cancer. Although the chelation of Zn^{2+} is well known, its removal from a protein in the presence of potential competing biologically relevant ions such as Cu^{2+} is hardly explored. Herein we present a peptoid – N-substituted glycine trimer – incorporating a picolyl group at the N-terminus, a non-coordinating but structurally directing benzyl group at the C-terminus and a 2,2′:6′,2″-terpyridine group in the second position, that selectively binds Zn^{2+} ions in the presence of excess Cu^{2+} ions in water. We further demonstrate that this chelator can selectively bind Zn^{2+} from a pool of excess biologically relevant and competitive ions (Cu^{2+}, Fe^{3+}, Ca^{2+}, Mg^{2+}, Na^{+}, and K^{+}) in a simulated body fluid (SBF), and also its ability to remove Zn^{2+} from a natural zinc protein domain (PYK**C**PE**C**GKSFSQKSDLVK**H**QRT**H**TG) in a SBF.

Introduction

The metal ion Zn^{2+} plays an important role in several enzymes and transcription factors within the human body, where it acts as a structural co-factor by allowing the protein to fold into a stable conformation, thus enabling a specific function.[1] Zinc finger proteins (ZFPs), 3% in abundance among the entire human genome, are a common DNA binding motif in transcription factors.[2] Recent reports indicate extensive participation of ZFPs in several diseases, such as parasitic diseases,[3] cancer,[4] viral contamination[5] or even neurological problems.[6] Therefore ZFPs are increasingly recognized as therapeutic targets.[2] The approach for treating diseases by targeting ZFPs is mainly associated with the replacement and/or removal of Zn^{2+} from the protein scaffold; proteins lacking Zn^{2+} would become apo-proteins (Scheme 1), will not be able to bind the nucleotide, and eventually would become inactive.[7] One approach to obtain an apo-protein is by replacing Zn^{2+} with other metal ions.[2] Although this strategy is well explored, it can lead to possible side effects from the substituting metal ions. Thus, removal of Zn^{2+} from ZFPs (unstructured protein, shown in blue in Scheme 1) by using an unbound chelator specific to zinc (shown in cyan in Scheme 1) to form an un-structured apo-protein (shown in grey, Scheme 1) would be advantageous. The major challenge related to Zn^{2+} extraction is the development of water-soluble small molecular probe-based chelators that could bind Zn^{2+} in competition with a strong opponent such as Cu^{2+}; even molecules that are routinely used to chelate zinc, *e.g.* ethylenediaminetetraacetic acid (EDTA) and *N*,*N*,*N*′,*N*′-tetrakis(2-pyridylmethyl)ethylenediamine (TPEN) are not selective to Zn, and this limits their utilization.[8a]

Only a handful of examples of peptidomimetics are known for Zn^{2+} chelation.[8b–d] Most of these examples, however, do not consider the binding of Zn^{2+} in the presence of other biologically relevant ions including Ca^{2+}, Mg^{2+}, Na^{+}, K^{+} and especially Cu^{2+}, which is the binding competitor of Zn^{2+}. It was previously reported that a cytochrome-based assembly can bind Zn^{2+} in the presence of Ni^{2+}, Co^{2+} or Cu^{2+}; however, this assembly was not selective to Zn^{2+}, as it was also binding the other metal ions.[8d] Moreover, selective binding to Zn^{2+} was tested neither in a mixture of different metal ion competitors nor in an environment similar to body fluids such as blood plasma (*i.e.*; in the presence of other ions such as Cl^{-}, HCO_3^{-}, HPO_4^{2-} *etc.*).[9] In such a fluid, the Cu^{2+}/Zn^{2+} concentration ratio can range between 1.06 (ref. 9c) to 1.39.(ref. 9d) Therefore, only the

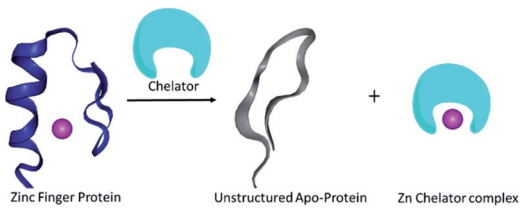

Scheme 1 A schematic representation of Zn^{2+} chelation from a structured ZFP domain (shown in blue) by using a suitable chelator resulting in an unstructured apo-protein (shown in grey).

Schulich Faculty of Chemistry, Technion-Israel Institute of Technology, Technion City, Haifa 3200008, Israel. E-mail: gm92@technion.ac.il

† Electronic supplementary information (ESI) available: Detailed synthetic procedures of the peptoid and Zn^{2+} and/or Cu^{2+} complexes, UV-Vis measurements, ESI-MS analysis, coordinates of the geometry optimized configuration of Zn^{2+} and Cu^{2+} complexes with the peptoid. See DOI: 10.1039/d0sc03391j

exclusive selectivity to Zn^{2+} over Cu^{2+} chelation within such ratios would be adequate for therapeutic applications.

Peptoids, N-substituted glycine oligomers, are peptidomimetics akin to peptides that are composed of primary amines instead of amino acids. Due to their ease of synthesis on a solid support,[10] sequence versatility and high stability, they exhibit great potential for application in catalysis,[11] self-assembly,[12] metal binding[13] and recognition,[14] and medicine.[15] Compared to small molecule chelators, peptoid chelators are advantageous because various metal-binding ligands and structural elements of choice can be incorporated within their scaffold with high sequence specificity, leading to control over a desired coordination geometry and complex stability. They include different N-donor ligands, many of which are the basis for systems used for Zn^{2+} chelation and/or sensing.[16] Indeed, peptoids bearing the N-donor ligands 8-hydroxyquinoline (HQ) and imidazole, can bind Zn^{2+} (among other metal ions).[13d,8e] Moreover, peptoids having imidazole groups were shown to bind Zn^{2+} more efficiently than peptoids having thiols as ligands.[8e] The N-donor ligand 2,2′:6′,2″-terpyridine (terpy) was incorporated together with HQ within a helical peptoid hexamer in a sequence-specific manner, resulting in selective intermolecular binding of Zn^{2+} by two terpy ligands.[14b] Other N-donor ligands that were successfully incorporated within peptoids are 2,2′-bipyridine,[13a] and 1,10-phenanthroline,[13c] but they were not used as Zn^{2+} chelators. Based on our achievements in the area of metallopeptoids, we prepared a series of water-soluble peptoid trimers, and found that one of these trimers can bind Zn^{2+} selectively from a mixture containing metal ion competitors including Cu^{2+} in a Cu^{2+}/Zn^{2+} concentration ratio that exists in human body fluids. Significantly, we demonstrated successful chelation and extraction from a zinc finger protein.

Results and discussion

Design and synthesis of a Zn^{2+}-peptoid chelator

In general, quinolone-based Zn^{2+} probes suffer from poor solubility and/or low cell permeability.[17] Thus, although HQ-based peptoids were shown to bind Zn^{2+}, HQ might not be a good choice for our current peptoid design. On the other hand, fluorescence studies with terpy-based ligands, which were carried out in a solution containing either Zn^{2+} or Cu^{2+}, demonstrated the ability of terpy to bind Zn^{2+} but not Cu^{2+}. Significantly, it was shown that in an aqueous solution, the association constant of terpy for Zn^{2+} is much higher than that for Cu^{2+}, suggesting that terpy has a higher affinity for Zn^{2+} in comparison with Cu^{2+}.[18] Additionally, the role that terpy plays in various metallo-intercalating drugs (where terpy helps to increase the DNA-binding ability),[19] stands for its utility as a biocompatible compound, making it the preferred choice as a chelating unit in the design of biomimetic chelators. As terpy is a tridentate ligand, and Zn can be stabilized *via* a tetra, penta or hexa-coordination, it is indeed required to incorporate a co-ligand that will stabilize an intramolecular 1 : 1 Zn : peptoid complex. This is because intramolecular metallopeptoid complexes were shown to have greater stability than their equivalent intermolecular metallopeptoid complexes, as evident from their higher association constants.[20] As the most common coordination number of Zn^{2+} complexes is four,[21] we chose to incorporate as the co-ligand a picolyl group (Npam), another N-donor metal-binding moiety[22] preferable for Zn^{2+} chelation.[8e] We previously showed that a non-coordinating bulky side chain incorporated next to an active site within the peptoid scaffold has an important role as a structure-directing group, and facilitates the peptoid's activity.[11] As the terpy and picolyl groups are anticipated to form a distinct coordination site, we sought to incorporate a non-coordinating group next to it and explore its effect on Zn^{2+} binding. To this aim, we incorporated one additional aromatic[23] or aliphatic[24] non-coordinating side chain at the C-terminus of the peptoid. Thus, peptoids **PT-1** to **PT-7** bearing a benzyl, naphthyl, cyclohexyl, (*R*)-(−)-3,3-dimethyl-2-butyl, pentyl, allyl and 2-methoxyethyl group, respectively (Fig. 1 and S2†), were synthesized and characterized. In addition, the peptoid dimer **PD-1**, which lacks the non-coordinating group, was synthesized as a control (Fig. 1). All the peptoids were synthesized by the sub-monomer approach on resin,[10] cleaved, purified by HPLC and lyophilized to obtain the pure peptoid products (>95% purity). The mass of the peptoids as determined by ESI-MS was consistent with their sequences (Fig. S3–S12† for HPLC and Fig. S13–S22 for ESI-MS, ESI†).

Binding of Zn^{2+} and Cu^{2+} to the peptoids PT1–PT7 and PD-1 in water

The peptoids **PT1–PT7** and **PD-1** are soluble in water and thus UV-Vis characterization has been carried out in a non-buffered water solution. Metal free **PT-1** exhibits absorbance maxima at 235 and 275 (with a small hump at 262) nm in a water medium arising from the ligands terpy and picolyl, respectively. Upon addition of zinc acetate, the bands near 235 and 275 nm shifted to 244 and 274 nm respectively, and new absorption bands near $\lambda = 310$ and 322 nm were produced (Fig. 2a). A metal-to-peptoid ratio plot constructed from these UV-Vis titrations was consistent with the 1 : 1 peptoid : Zn^{2+} ratio, demonstrating the formation of the intramolecular complex Zn**PT-1** (Fig. 2a, inset). Addition of 1 equiv. of copper(II) acetate to **PT-1** produced new bands near $\lambda = 315$ and 328 nm (Fig. 2b and S23b†). The difference between the UV spectra of the two complexes Zn**PT-1** and Cu**PT-1** enables the detection of the coordination of one of these ions over the other in competition experiments followed by UV-Vis analysis. Indeed, the UV-Vis spectrum of **PT-1** with

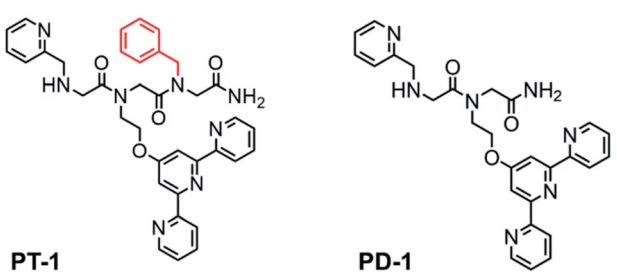

Fig. 1 Chemical structures of peptoids PT-1 and PD-1.

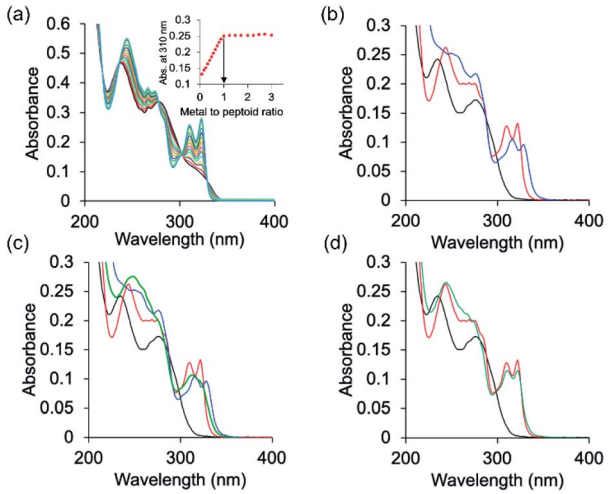

Fig. 2 UV-Vis spectra of (a) **PT-1** titration with Zn^{2+}. **PT-1** (17 μM) in water was titrated with 2 μL aliquots of metal ions (2 mM in H_2O) in multiple steps (black = free peptoid **PT-1** and blue = metal complex). Inset: metal-to-peptoid ratio plot for Zn^{2+} binding to **PT-1**. (b) Zn^{2+} added to **PT-1** (red line) and Cu^{2+} added to **PT-1** (blue line), (c) competition experiment between Zn^{2+} and Cu^{2+} with **PT-1** in a 1 : 3 Zn^{2+} : Cu^{2+} ratio (black: **PT-1**; red: **PT-1** with Zn^{2+}; blue: **PT-1** with Cu^{2+}; green: **PT-1** with 1 : 3 Zn^{2+} : Cu^{2+}) and (d) competition experiment between Zn^{2+} and Cu^{2+} with **PT-1** in a 1 : 2 Zn^{2+} : Cu^{2+} ratio (black: **PT-1**; red: **PT-1** with Zn^{2+}; green: **PT-1** with 1 : 2 Zn^{2+} : Cu^{2+}), (8 μM in b–d, solvent: water).

a mixture of Zn^{2+} and Cu^{2+} in a 1 : 4 ratio was obtained, revealing an expected selective chelation of Cu^{2+} over Zn^{2+} (see Fig. S24a† for UV-Vis and Fig. S26b† for ESI-MS).

This selectivity decreases in a 1 : 3 Zn^{2+} : Cu^{2+} ratio (Fig. 2d and S26a† for ESI-MS) and is, remarkably, completely lost and actually turns to selectivity towards Zn^{2+} in a 1 : 2 Zn^{2+} : Cu^{2+} ratio (Fig. 2c and S25a† for ESI-MS). A sample taken from this UV-Vis solution was subjected to ESI-MS analysis and the results supported chelation of zinc only, as evident from the well-matched ESI-MS pattern of simulated and experimental data (Fig. S25†). In Fig. 2a, which shows the titration of **PT-1** with Zn^{2+}, we could identify five isosbestic points, *i.e.*; 218, 236, 278, 300 and 329 nm. The points near 218 and 329 nm do not show much change in the absorbance value before and after metal binding, and the isosbestic point near 278 nm is common for both metal ions. Therefore, we considered the points near 236 and 300 nm for explaining the metal binding. In a 1 : 4 (Zn^{2+} : Cu^{2+}) ratio, the UV signal is similar to that of Cu^{2+} and there is no similarity in isosbestic points to those of the Zn^{2+} signal. In a 1 : 3 (Zn^{2+} : Cu^{2+}) ratio, the UV signal passes through the 300 nm isosbestic point only and other points are not similar to those of both Zn^{2+} and Cu^{2+}, which explains the binding of both Zn^{2+} and Cu^{2+} to **PT-1**. However in a 1 : 2 (Zn^{2+} : Cu^{2+}) ratio, the UV signal passes through 235 and 300 nm isosbestic points which explains the binding of Zn^{2+} only with **PT-1** (supported by mass spectrometric analysis).

The role of the non-coordinating group that was incorporated at the C-terminus was examined by conducting competition experiments similar to the experiment that was carried out with **PT-1**. Thus, each of the peptoids **PT-2** to **PT-7** and **PD-1** was mixed with a 1 : 2 Zn^{2+} : Cu^{2+} solution in water, and the solutions were analyzed by UV-Vis spectroscopy. Interestingly, the spectra of these solutions indicated that all these peptoids do not bind Zn^{2+} but rather bind Cu^{2+} (Fig. S27 and S33, ESI†). To understand this result, the dissociation constants of peptoids **PT-1** to **PT-3** with Zn^{2+} were measured by a competition experiment with EDTA at pH 7. The dissociation constant of **PT-1** was found to be 1.85×10^{-13} M (Fig. S31†), 1.4–2.4 times lower than that of **PT-2** (2.65×10^{-13} M, Fig. S31†) and **PT-3** (4.5×10^{-13} M, Fig. S31†), and about 10 times lower than its dissociation constant with Cu^{2+} (2.2×10^{-12} M, Fig. S31†). The results from all the above experiments suggest that a non-coordinating structure-directing group is required to achieve selective binding of Zn^{2+} to the terpy/picolyl coordination site, but that such a group should not be too bulky to hinder the binding. Among the seven non-coordinating groups studied here, the benzyl side chain is the best one to function as a non-hindering structure-directing group and assists the coordinating ligands to selectively bind Zn^{2+} over Cu^{2+}. Hence, this non-coordinating group provides the advantages of a second coordination sphere around the binding site, similar to the one afforded by the folds within the active site of functional proteins.

We have previously showed that the N terminal –NH group of metal-binding peptoids can coordinate Cu^{2+}.[12,13a] We therefore anticipated that acetylating the N-terminal of **PT-1** will enable the minimization of the possibility of Cu^{2+} binding, and increase the selectivity towards Zn^{2+} even with Zn^{2+} : Cu^{2+} ratios higher than 1 : 3. Thus, **PT-1** was re-synthesized and its N-terminus has been acetylated to obtain **PT-1Ac** (Fig. 3). This peptoid was mixed with a 1 : 2 Zn^{2+} : Cu^{2+} solution in water, followed by UV-Vis spectroscopy. Despite our expectations, the resulting spectrum indicated that acetylation at the N-terminal cannot improve the selectivity, as **PT-1Ac** failed to bind Zn^{2+} in the presence of two equivalents of Cu^{2+}. These results also suggest that the N-terminal secondary amine has a role in the selectivity of **PT-1** for Zn^{2+}.

To establish the role of the picolyl group in the selective binding to Zn^{2+}, we have also synthesized **PT-8**, which incorporates a benzyl group instead of the picolyl side chain (Fig. 3). A similar competition experiment performed with a 1 : 2 Zn^{2+} : Cu^{2+} solution followed by UV-Vis spectroscopy revealed that **PT-8** binds Cu^{2+} rather than Zn^{2+}, indicating that the picolyl side chain is also required for selectivity to Zn^{2+} in the presence of excess Cu^{2+} in solution (Fig. 4). A similar competition experiment performed with a 1 : 1 mixture of terpy and picolyl amine in acetonitrile solution also demonstrated selectivity to Cu^{2+} only.

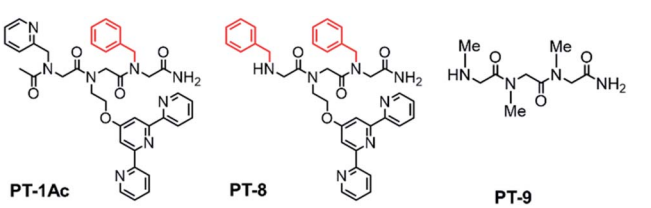

Fig. 3 Additional peptoid oligomers designed and synthesized for this study.

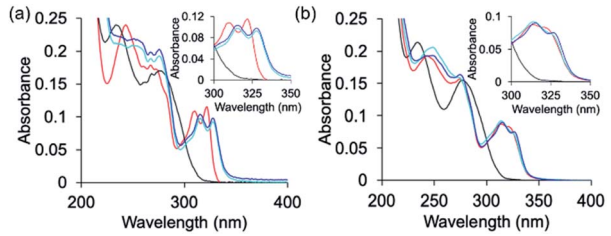

Fig. 4 UV-Vis spectra describing the competition between Zn^{2+} and Cu^{2+} in peptoid binding. The spectra were recorded upon addition of a 1 : 2 Zn^{2+} : Cu^{2+} mixture (8 μM in water) to (a) PT-1Ac and (b) PT-8 (black: Peptoid, red: Zn^{2+} complex, blue: Cu^{2+} complex and cyan: mixture).

Overall, the competition experiments with peptoids **PT-2** to **PT-8**, **PD-1** and **PT-1Ac**, as well as with a mixture of the two ligands, with 1 : 2 Zn^{2+} : Cu^{2+} (Fig. S38, ESI†), collectively established **PT-1** as a unique chelator for Zn^{2+}, which can bind it selectively from a solution containing an excess of up to 3 equiv. of Cu^{2+}.

Exploring the selectivity of PT-1 towards Zn^{2+} in solutions containing various other metal ions

To explore the ability of **PT-1** to bind Zn^{2+} selectively from a pool of other biologically relevant metal ions, **PT-1** was titrated with 1 equiv. of Ca^{2+}, K^{+}, Mg^{2+}, Na^{+} or Fe^{3+} in a non-buffered water solution followed by UV-Vis measurements. The results suggested no interaction between the examined metal ions and **PT-1**, as no shift in the absorbance bands was recorded and the UV-Vis spectra were mostly identical before and after the titration (Fig. S57, ESI†). The chelation of biologically relevant metal ions, however, does not take place in water or buffered solutions but rather in a human body fluid. Thus, we have prepared a simulated body fluid (SBF) according to a previously reported method[25] and tested the chelation of Zn^{2+} and Cu^{2+} by **PT-1** in this SBF solution. The complexation of both Zn^{2+} and Cu^{2+} was successful in the SBF (Fig. S58†), indicating that **PT-1** is a good chelator of these ions in the SBF also. The stability of Zn**PT-1** was monitored by a 24 hour UV-Vis measurement in the SBF at 37 °C and the obtained spectrum matched the one measured in water, suggesting that Zn**PT-1** maintains its stability in a SBF. To further explore the selectivity of **PT-1** towards Zn^{2+} in the SBF, competition experiments between Zn^{2+}, Cu^{2+}, Fe^{3+}, Ca^{2+}, Mg^{2+}, Na^{+}, and K^{+} in varying ratios were performed. Initially, two mixture solutions were prepared, in which the ratio between Zn^{2+} and Cu^{2+} was varied between 1 : 2 and 1 : 3, while keeping the other metal ions in excess owing to their abundance in the human body with respect to Zn^{2+}.[26] Both **PT-1** and the two mixtures (A with the Zn^{2+} : Cu^{2+} : Fe^{3+} : Ca^{2+} : Mg^{2+} : Na^{+} : K^{+} ratio 1 : 2 : 5 : 10 : 10 : 10 : 10 and B with the ratio 1 : 3 : 5 : 10 : 10 : 10 : 10) were prepared in the SBF. Each mixture was added to **PT-1** in two different UV-Vis experiments and the spectra were recorded. Absolute selectivity towards Zn^{2+} was observed upon addition of mixture A (Fig. S59, ESI†), consistent with the results obtained in the competition experiment between Zn^{2+} and Cu^{2+} in binding to **PT-1** (Fig. 2d).

Characterization of the ZnPT-1 and CuPT-1 complexes

To understand the ability of **PT-1** to selectively bind Zn^{2+} over Cu^{2+} we have characterized both complexes Zn**PT-1** and Cu**PT-1** and analyzed the structural differences between them, specifically the coordination geometries about their metal center. To this aim, Zn**PT-1** and Cu**PT-1** complexes were prepared under different reaction conditions and characterized by UV-Vis spectroscopy, ESI-MS, IR spectroscopy, EPR (Cu**PT-1**) and ^{1}H NMR (Zn**PT-1**), and their possible coordination geometries were computed by density-functional theory (DFT) calculations. Initially, the two complexes were prepared by mixing **PT-1** in water with the acetate salt of either Zn^{2+} or Cu^{2+} in an exact 1 : 1 peptoid : metal ratio, for 4 hours in a non-buffered water solution at room temperature. After 4 hours, the solutions were analyzed by UV-Vis spectroscopy and ESI-MS. The UV-Vis spectra were identical to those obtained from the titration experiments and the MS analysis confirmed the formation of the Zn**PT-1** and Cu**PT-1** complexes, suggesting coordination to the acetate counter ion (Fig. S43 and 44,† ESI†). The solutions were than lyophilized to obtain the solid complexes Zn**PT-1** and Cu**PT-1** (92% and 88% yield, respectively). To test the stability of these complexes with time, the same reactions were performed but the reaction mixtures were allowed to stir for 24 hours at room temperature. The samples from these solutions were analyzed by UV-Vis spectroscopy every several hours and the spectra in all the cases were almost identical to the ones recorded after 4 hours, indicating high complex stability over time. Additionally, the same reactions were also performed in water at 35 °C and 50 °C for 24 hours. The samples taken from these mixtures after 24 hours were analyzed by UV-Vis spectroscopy. These spectra also showed a similar absorbance signal with almost no change in the UV-Vis signal intensity compared to that of the spectra obtained from the solutions that were mixed at room temperature (Fig. S45–46, ESI†). These results imply that the formed complexes are both kinetic and thermodynamic products. Finally, the absorbance signal of the complexes was measured when the reactions were performed at room temperature for four hours in methanol or acetonitrile as the solvent, showing UV-Vis spectra nearly similar to those obtained when the reactions were performed in water. These findings suggest that Zn^{2+} and Cu^{2+} complex formation does not depend on one coordinating solvent or another.

For further insight, ^{1}H-NMR of the **PT-1** and its Zn^{2+} complex was carried out in solution. We note here, that assigning the ^{1}H-NMR chemical shift of the peptoids is not straightforward because peptoids adopt multiple conformations in solution caused by *cis–trans* interconversions at the backbone amides, and because there are no intramolecular CO–HN hydrogen bonds, which collectively result in highly flexible scaffolds.[27] Indeed, the NMR spectra of **PT-1** and Zn**PT-1** in water were too broad to analyze, and possible interaction of the N-terminal –NH group with the metal center could not be detected due to proton exchange with the solvent. Thus, in order to be able to assign the ^{1}H-NMR chemical shift of **PT-1** and its zinc complex, we synthesized the complex by mixing 1 equiv. of **PT-1** with one equiv. of zinc acetate dihydrate in deuterated acetonitrile and

performed both measurements of **PT-1** and Zn**PT-1** in this solvent. In addition, we have designed the peptoid trimer **PT-9** (Fig. 3), having three methyl side chains, as a simple model that can represent the scaffold of **PT-1** in ^{1}H-NMR analysis. **PT-9** was synthesized on a solid support *via* the submonomer method, cleaved and purified by HPLC (>95% purity), and its identity was confirmed by ESI-MS. The ^{1}H-NMR spectrum of **PT-9** in acetonitrile exhibits four groups of signals; among them a small broad signal at 9 ppm that can be assigned to the proton of the N-terminal –NH group, a multiplet in the 5.8–7 ppm region assigned to the two protons of the $-NH_2$ group at the C-terminal, and a multiplet in the region between 3.7 and 4.4 ppm corresponding to the prochiral geminal protons in the glycine-like backbone are observed (Fig. S49†). In addition, the ^{1}H-NMR spectra of benzylamine, 2,2′:6′,2″-terpyridine and 2-picolyl amine were measured in acetonitrile and the signals were fully assigned (Fig. S50–52, ESI†).

With these spectra in hand, we performed ^{1}H-NMR measurements on **PT-1** and its corresponding 1 : 1 Zn^{2+} complex in acetonitrile and analyzed the obtained spectra based on the ^{1}H-NMR data of **PT-9** and the three side chains (Fig. 5). In general, the NMR signals of both the peptoid and its zinc complex appear as groups of multiplets between 7.75 ppm and 9 ppm, between 7.2 and 7.6 ppm, in the range of 5.8–6.7 ppm, between 4.3 and 4.6 ppm and about 3.8–4.2 ppm (Fig. 5a and b). The NMR spectrum of **PT-1** exhibits: (1) a broad signal at 9.2 ppm that we assigned to the N-terminal –NH proton, together with a multiplet near 9.18 ppm that is assigned to three α-protons adjacent to pyridine nitrogen, (2) multiplets about 7.75–9 ppm ascribed to the protons of terpy and picolyl groups, (3) signals in the 7.2–7.6 ppm range assigned to the five protons of the benzyl group together with other less acidic aromatic protons from the pyridine-based ligands, (4) a multiplet in the 5.8–6.7 ppm region assigned to the two protons of the C-terminal $-NH_2$ group, and (5) signals in the 4.3–4.6 ppm and 3.8–4.2 ppm range that we ascribed to the protons of the skeletal methylene groups, and to the protons of the side-chain methylene linkers, respectively, a total of fourteen protons (Fig. S53, ESI† for a more detailed assignment). The NMR spectrum of Zn**PT-1** exhibits a downfield shift of the aromatic protons from the pyridine-based ligands (*e.g.*; proton signal near 7.9 ppm shifted to 8 ppm, 8 to 8.1 ppm, 8.25 ppm to 8.3 ppm, 9.18 to 9.20 ppm *etc.*, Fig. 5c), indicating the participation of terpy and picolyl in the zinc binding.[28] The lack of the terminal –NH signal could be attributed to either its coordination to Zn^{2+} or to some interactions with either water molecules or acetate ions from the zinc acetate dihydrate salt used for the complex formation.

To prove this point we have performed an FT-IR measurement on the zinc complex, which we have isolated from the acetonitrile solution, as well as on **PT-1**, in the solid state. The FT-IR data revealed that the bands corresponding to the –NH stretching in the range between 2700 and 3400 cm^{-1} are present in both spectra, indicating that the terminal –NH group is not coordinated to zinc (Fig. S54†).[13a,29a] Interestingly, the FT-IR spectrum of Zn**PT-1** exhibits bands near 1535 cm^{-1} and 1440 cm^{-1}, both assigned to COO^- stretching, with a $\Delta\nu(COO^-)$ = 95 cm^{-1}, suggesting a bidentate coordination of the acetate ligand to Zn^{2+} (Fig. S54†).[29b] This FT-IR spectrum was almost identical to the FT-IR spectrum of Zn**PT-1** formed in water.

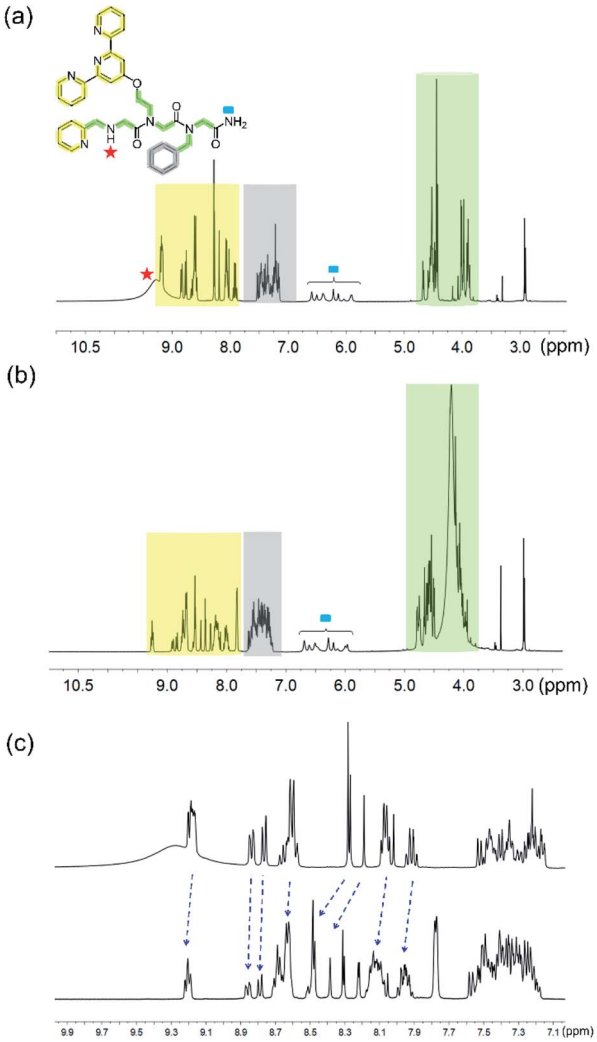

Fig. 5 ^{1}H-NMR (in 400 MHz) spectra of (a) **PT-1** and (b) Zn**PT-1**. (c) Expanded aromatic region of **PT-1** (top) and Zn**PT-1** (down) in CD_3CN; the changes are marked with blue arrows.

Based on our structural experimental data, we could suggest that within Zn**PT-1**, Zn^{2+} binds to the three nitrogen atoms of terpy, the nitrogen atom of picolyl, and the two oxygen atoms from one acetate molecule in a bidentate mode, forming a hexa-coordination geometry. To support this assumption, we computed this structure using DFT-D4.[30] Unrestricted DFT calculations resulted in a geometry-optimized conformation with a hexa-coordinated zinc center, including a bidentate coordination to the acetate ion in a distorted octahedral geometry (Fig. 6a and the ESI† for the coordinates).

To understand the selectivity of **PT-1** to Zn^{2+} in the presence of Cu^{2+}, we first characterized Cu**PT-1** *via* FT-IR and EPR spectroscopies. The FT-IR spectrum obtained from measuring a solid sample of Cu**PT-1** suggested that similar to Zn**PT-1**, there is no coordination of the terminal –NH group to copper. On the other hand, the FT-IR spectrum of Cu**PT-1** showed bands

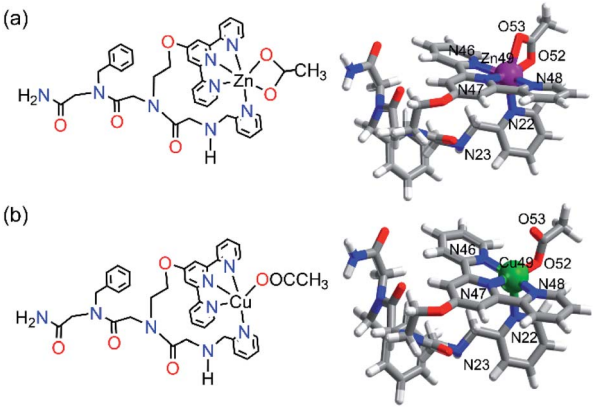

Fig. 6 Chemical structure representation and DFT-D4 energy optimized configurations of (a) Zn**PT-1** and (b) Cu**PT-1** (color code: grey: carbon, white: hydrogen, red: oxygen, blue: nitrogen, purple: zinc, and green: copper).

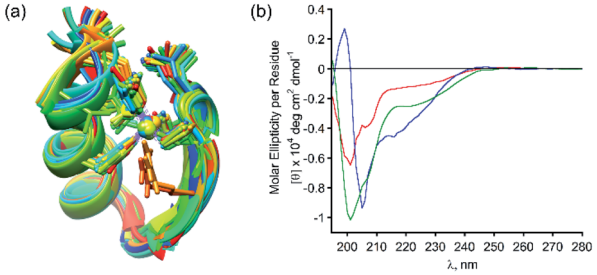

Fig. 7 (a) A 3D model graphic representation of a zinc finger protein (PDB accession code 1ZNF);[36] (b) CD spectra (at 100 μM SBF) of the apo-ZF (red line), Zn-ZF (blue line) and Zn^{2+} removed ZF (green line).

corresponding to $\upsilon_{asym}(COO^-)$ and $\upsilon_{sym}(COO^-)$ at 1593 cm^{-1} and 1420 cm^{-1}, respectively, leading to a $\Delta\upsilon(COO^-)$ of 173 cm^{-1}, which stands for a pseudo bridged uni-dentate arrangement of Cu^{2+} (Fig. S54b†).[31] The X-band EPR measurements were performed in a frozen solution, and the resulting experimental spectrum was simulated to obtain the Hamiltonian parameter as $g_{-II} = 2.22$; $g_{\perp} = 2.06$ and $A_{-II} = 165$ G. These parameters suggest that Cu**PT-1** adopts a square pyramidal geometry[32] about the copper center (Fig. S55†). Overall, these data suggest that within Cu**PT-1**, Cu^{2+} binds to the three nitrogen atoms of terpy, the nitrogen atom of picolyl, and one oxygen atom from one acetate molecule, forming a penta-coordination geometry. DFT-D4 calculations resulted in a geometry-optimized conformation with a square pyramidal copper center, including a mono-dentate linkage from the acetate ion (Fig. 6b and the ESI† for the coordinates). The calculated structures of Zn**PT-1** and Cu**PT-1** were utilized to investigate their relative stability based on the HOMO–LUMO gap, as the larger the energy difference between the HOMO and LUMO, the more stable is the complex.[33] Indeed, the HOMO–LUMO gap in Zn**PT-1** (4.313 eV) is higher than that in Cu**PT-1** (3.671 eV) suggesting the higher kinetic stability of Zn**PT-1** over Cu**PT-1**, which can explain the selectivity to Zn^{2+} (see the ESI†).

Utility of the peptoid chelator

Following our results showing high selectivity in the binding of Zn^{2+} by **PT-1**, we wished to explore the ability of **PT-1** to bind and remove Zn^{2+} from a Zn finger protein. To this aim, we chose the apo-zinc finger protein domain PYK**C**-PE**C**GKSFSQKSDLVK**H**QRT**H**TG (ZF), because it has canonical two cysteines and two histidines, which form a CCHH type metal coordination site (Fig. 7a).[34] Initially the circular dichroism spectrum of the apo-ZF was measured in acetate buffer (pH 6.5) in order to compare it to a previously reported spectrum (Fig. S62†).[35] The CD spectrum of the unstructured apo protein has a minimum near 200 nm, demonstrating its random coil conformation. The CD spectrum of the zinc complex of this protein exhibits a maximum at 190 nm and double minima near 205 and 218 nm, suggesting the formation of a structured α-helical conformation. Upon addition of **PT-1** in acetate buffer at pH 6.5, the minima shift back to 200 nm, suggesting the successful chelation of Zn^{2+} from the domain of the ZF. ESI-MS measurements of the zinc-bound protein before and after the addition of **PT-1** support the extraction of Zn^{2+} from the protein by **PT-1** (see the ESI†). This chelation experiment was repeated in a SBF followed by CD measurements. The spectrum corresponding to the apo-ZF exhibits a minimum near 200 nm, which changes after the addition of Zn^{2+}, showing a maximum at 190 nm and double minima near 205 and 218 nm. This spectrum changes again after the addition of **PT-1**, exhibiting only one minimum near 200 nm (Fig. 7b). These results establish the ability of the peptoid chelator **PT-1** to bind Zn^{2+} from the zinc finger protein in a biological-like medium that contains ions such as Cl^-, HCO_3^-, SO_4^{2-}, HPO_4^{2-}, Na^+, Ca^{2+}, K^+ and Mg^{2+} at a concentration similar to that of our body fluid.[25]

Conclusions

Controlling chelation processes for the development of therapeutics that target specific metal ion(s) remains a great challenge in chemistry and chemical biology. Although small molecular probes incorporating bidentate and/or tridentate ligands, as well as peptidomimetic oligomers with tunable sequences were developed for Zn^{2+} chelation, competitive binding in the presence of other biologically relevant ions such as Cu^{2+} in an aqueous medium is scarce. Herein we combined the advantages from both systems, and by capitalizing on the water solubility of short peptoids, we rationally designed for the first time a water-soluble peptoid trimer chelator, **PT-1**, bearing the ligands terpy and picolyl, that can selectively bind Zn^{2+} in the presence of other biologically relevant and competitive ions in water, as well as in a simulated body fluid (SBF). The chelation of Zn^{2+} ions and their main metal ion competitor Cu^{2+} by **PT-1** was investigated using several spectroscopic studies and the coordination geometry of both complexes Zn**PT-1** and Cu**PT-1** was further studied by DFT-D4 calculations. The selectivity of **PT-1** towards Zn^{2+} was rationalized based on the theoretical analysis. Finally we could show that PT-1 can extract Zn^{2+} from a Zn-finger protein domain in a SBF. These results open up

a new avenue for the design of zinc chelators as a therapeutic approach targeting zinc finger proteins, towards multidirectional research in chemistry, biology and medicine.

Conflicts of interest

There are no conflicts to declare.

Acknowledgements

The authors thank Dr Boris Tumanskii from the Schulich Faculty of Chemistry for the EPR measurements and analysis and Mrs Larisa Panz from the Schulich Faculty of Chemistry for the MS measurements and analysis. PG thanks the Lady Davis Trust for his postdoctoral fellowship. This work was funded by the Israel Science Foundations, grant # 395/16 awarded to Prof. Galia Maayan.

Notes and references

1 (*a*) A. I. Anzellotti and N. P. Farrell, *Chem. Soc. Rev.*, 2008, **37**, 1629–1651; (*b*) M. Cassandri, A. Smirnov, F. Novelli, C. Pitolli, M. Agostini, M. Malewicz, G. Melino and G. Raschellà, *Cell Death Discovery*, 2017, **3**, 17071, DOI: 10.1038/cddiscovery.2017.71; (*c*) T. V. O'Halloran, *Science*, 1993, **261**, 715–725.

2 C. Abbehausen, *Metallomics*, 2019, **11**, 15–28.

3 N. G. Kolev, E. Ullu and C. Tschudi, *Cell. Microbiol.*, 2014, **16**, 482–489.

4 S. Vyas and P. Chang, *Nat. Rev. Cancer*, 2014, **14**(7), 502–509.

5 N. Iraci, O. Tabarrini, C. Santi and L. Sancineto, *Drug Discovery Today*, 2018, **23**(3), 687–695.

6 Y. Sun, D. Hu, J. Liang, Y. P. Bao, S. Q. Meng, L. Lu and J. Shi, *Schizophr. Res.*, 2015, **162**(1–3), 124–137.

7 (*a*) Y. M. Lee, Y. Duh, S. T. Wang, M. M. C. Lai, H. S. Yuan and C. Lim, *J. Am. Chem. Soc.*, 2016, **138**(11), 3856–3862; (*b*) Y. M. Lee, Y.-T. Wang, Y. Duh, H. S. Yuan and C. Lim, *J. Am. Chem. Soc.*, 2013, **135**, 14028–14031.

8 (*a*) E. Kawabata, K. Kikuchi, Y. Urano, H. Kojima, A. Odani and T. Nagano, *J. Am. Chem. Soc.*, 2005, **127**(3), 818–819; (*b*) A. Balliu and L. Baltzer, *ChemBioChem*, 2017, **18**(14), 1408–1414; (*c*) E. M. Nolan, J. W. Ryu, J. Jaworski, R. P. Feazell, M. Sheng and S. J. Lippard, *J. Am. Chem. Soc.*, 2006, **128**(48), 15517–15528; (*d*) J. D. Brodin, A. M. Morales, T. Ni, E. N. Salgado, X. I. Ambroggio and F. A. Tezcan, *J. Am. Chem. Soc.*, 2010, **132**, 8610–8617; (*e*) B. C. Lee, T. K. Chu, K. A. Dill and R. N. Zuckermann, *J. Am. Chem. Soc.*, 2008, **130**, 8847–8855.

9 (*a*) N. F. Zakharchuk, G. S. Soldatova, T. V. Novikova and N. S. Borisova, *Chem. Sustainable Dev.*, 2006, 231–240; (*b*) W. I. Mortada, I. M. M. Kenawy, A. M. Abdelghany, A. M. Ismail, A. F. Donia and K. A. Nabieh, *Mater. Sci. Eng. Carbon*, 2015, **52**, 288–296; (*c*) J. Weissgarten, S. Berman, R. Bilchinsky, D. Modai and Z. Averbukh, *Metabolism*, 2001, **50**, 270–276; (*d*) L. J. Hinks, B. E. Clayton and R. S. Lloyd, *J. Clin. Pathol.*, 1983, **36**, 1016–1021.

10 R. N. Zuckermann, J. M. Kerr, W. H. Moosf and S. B. H. Kent, *J. Am. Chem. Soc.*, 1992, **114**, 10646–10647.

11 (*a*) K. J. Prathap and G. Maayan, *Chem. Commun.*, 2015, **51**(55), 11096–11099; (*b*) D. C. Mohan, A. Sadhukha and G. Maayan, *J. Catal.*, 2017, **355**, 139–144; (*c*) T. Ghosh, P. Ghosh and G. Maayan, *ACS Catal.*, 2018, **8**(11), 10631–10640.

12 T. Ghosh, N. Fridman, M. Kosa and G. Maayan, *Angew. Chem., Int. Ed.*, 2018, **57**(26), 7703–7708.

13 (*a*) M. Baskin and G. Maayan, *Dalton Trans.*, 2018, **47**(31), 10767–10774; (*b*) M. Baskin and G. Maayan, *Biopolym*, 2015, **104**(5), 577–584; (*c*) H. Tigger-Zaborov and G. Maayan, *J. Colloid Interface Sci.*, 2017, **508**, 56–64; (*d*) L. Zborovsky, A. Smolyakova, M. Baskin and G. Maayan, *Chem. – Eur. J.*, 2018, **24**(5), 1159–1167; (*e*) L. Zborovsky, H. Tigger-Zaborov and G. Maayan, *Chem. – Eur. J.*, 2019, **25**(38), 9098–9107.

14 (*a*) M. Baskin, H. Zhu, Z. W. Qu, J. H. Chill, S. Grimme and G. Maayan, *Chem. Sci.*, 2019, **10**(2), 620–632; (*b*) M. Baskin and G. Maayan, *Chem. Sci.*, 2016, **7**(4), 2809–2820; (*c*) M. Baskin, L. Panz and G. Maayan, *Chem. Commun.*, 2016, **52**, 10350–10353; (*d*) A. D. ' Amato, P. Ghosh, C. Costabile, G. Della Sala, I. Izzo, G. Maayan and F. De Riccardis, *Dalton Trans.*, 2020, **49**(18), 6020–6029.

15 J. A. Schneider, T. W. Craven, A. C. Kasper, C. Yun, M. Haugbro, E. M. Briggs, V. Svetlov, E. Nudler, H. Knaut and R. Bonneau, *Nat. Commun.*, 2018, **9**(1), 1–10, DOI: 10.1038/s41467-018-06845-3.

16 (*a*) F. Qian, C. Zhang, Y. Zhang, W. He, X. Gao, P. Hu and Z. Guo, *J. Am. Chem. Soc.*, 2009, **131**(4), 1460–1468; (*b*) H. W. Rhee, H. Y. Choi, K. Han and J. I. Hong, *J. Am. Chem. Soc.*, 2007, **129**(15), 4524–4525; (*c*) K. Komatsu, K. Kikuchi, H. Kojima, Y. Urano and T. Nagano, *J. Am. Chem. Soc.*, 2005, **127**(29), 10197–10204; (*d*) X. A. Zhang, D. Hayes, S. J. Smith, S. Friedle and S. J. Lippard, *J. Am. Chem. Soc.*, 2008, **130**(47), 15788–15789; (*e*) E. Kawabata, K. Kikuchi, Y. Urano, H. Kojima, A. Odani and T. Nagano, *J. Am. Chem. Soc.*, 2005, **127**(3), 818–819; (*f*) Z. Xu, K. H. Baek, H. N. Kim, J. Cui, X. Qian, D. R. Spring, I. Shin and J. Yoon, *J. Am. Chem. Soc.*, 2010, **132**(2), 601–610; (*g*) Y. Zhang, X. Guo, W. Si, L. Jia and X. Qian, *Org. Lett.*, 2008, **10**(3), 473–476; (*h*) P. Du and S. J. Lippard, *Inorg. Chem.*, 2010, **49**(23), 10753–10755; (*i*) W. Lin, D. Buccella and S. J. Lippard, *J. Am. Chem. Soc.*, 2013, **135**(36), 13512–13520.

17 X. Wang, and X. Chen, *Novel Nanomaterials for Biomedical, Environmental, and Energy Applications*, Elsevier, 2018.

18 (*a*) A. Mandal, A. Maity, S. Bag, P. Bhattacharya, A. K. Das and A. Basak, *RSC Adv.*, 2017, **7**(12), 7163–7169; (*b*) Z. Huang, J. Du, J. Zhang, X. Q. Yu and L. Pu, *Anal. Methods*, 2012, **4**(7), 1909–1912.

19 (*a*) P. Collery, *Proceedings of the Fourth International Symposium on Metal Ions in Biology and Medicine*, ed. P. Collery, J. Corbella, J. L. Domingo, J-C. Etienne and J. M. Llobet, John Libbey Eurotext, 1996, vol. 4, pp. 703–1996; (*b*) J. Gao, J. H. Reibenspies and A. E. Martell, *J. Inorg. Biochem.*, 2003, **94**, 272–278.

20 G. Maayan, M. D. Ward and K. Kirshenbaum, *Chem. Commun.*, 2009, 56–58.
21 M. J. Lachenmann, J. E. Ladbury, J. Dong, K. Huang, P. Carey and M. A. Weiss, *Biochem*, 2004, **43**(44), 13910–13925.
22 R. Zou, Q. Wang, J. Wu, J. Wu, C. Schmuck and H. Tian, *Chem. Soc. Rev.*, 2015, **44**(15), 5200–5219.
23 (*a*) J. R. Stringer, J. A. Crapster, I. A. Guzei and H. E. Blackwell, *J. Am. Chem. Soc.*, 2011, **133**(39), 15559–15567; (*b*) K. Kirshenbaum, A. E. Barron, R. A. Goldsmith, P. Armand, E. K. Bradley, K. T. V. Truong, K. A. Dill, F. E. Cohen and R. N. Zuckermann, *Proc. Natl. Acad. Sci. U. S. A.*, 1998, **95**(8), 4303–4308, DOI: 10.1073/pnas.95.8.4303; (*c*) C. M. Darapaneni, P. J. Kaniraj and G. Maayan, *Org. Biomol. Chem.*, 2018, **16**(9), 1480–1488.
24 C. W. Wu, K. Kirshenbaum, T. J. Sanborn, J. A. Patch, K. Huang, K. A. Dill, R. N. Zuckermann and A. E. Barron, *J. Am. Chem. Soc.*, 2003, **125**(44), 13525–13530.
25 T. Kokubo and H. Takadama, *Biomaterials*, 2006, **27**(15), 2907–2915.
26 F. B. Abdallah and T. R. Giffune, *Biochim. Biophys. Acta*, 2016, **1860**, 879–891.
27 (*a*) J. Karn, N. J. Keen, M. J. Churcher, F. Aboul-ela, G. Varani, F. Hamy, E. R. Felder, G. Heizmann and T. Klimkait, *Pharmacochem. Libr.*, 1998, **29**, 121–132; (*b*) C. M. Drapaneni, P. Ghosh, T. Ghosh and G. Maayan, *Chem. – Eur. J.*, 2020, **26**, 9573–9579.
28 E. Manandhar, J. H. Broome, J. Myrick, W. Lagrone, P. J. Cragg and K. J. Wallace, *Chem. Commun.*, 2011, **47**(31), 8796–8798.
29 (*a*) A. M. Díez-Pascual, *Polymers*, 2019, **11**(4), 625–630; (*b*) M. S. Ghazvini, G. Pulletikurthi, A. Lahiri and F. Endres, *ChemElectroChem*, 2016, **3**(4), 598–604.
30 (*a*) *TURBOMOLE, Version 7.3*, a development of University of Karlsruhe and Forschungszentrum Karlsruhe GmbH, 1989-2007, available from http://www.turbomole.com; (*b*) E. Caldeweyher, C. Bannwarth and S. Grimme, *J. Chem. Phys.*, 2017, **147**(3), 034112.
31 S. K. Papageorgiou, E. P. Kouvelos, E. P. Favvas, A. A. Sapalidis, G. E. Romanos and F. K. Katsaros, *Carbohydr. Res.*, 2010, **345**(4), 469–473.
32 (*a*) D. Floner, O. Lavastre, M. Zaarour, N. M. Saleh, F. Geneste, F. Justaud, R. Marion and N. A. Qachachi, *J. Inorg. Biochem.*, 2011, **105**(11), 1391–1397; (*b*) S. Muthuramalingam, K. Anandababu, M. Velusamy and R. Mayilmurugan, *Inorg. Chem.*, 2020, **59**(9), 5918–5928.
33 (*a*) Z. Zhou and R. G. Parr, *J. Am. Chem. Soc.*, 1990, **112**(15), 5720–5724; (*b*) J. I. Aihara, *J. Phys. Chem. A*, 1999, **103**(37), 7487–7495; (*c*) L. P. Ding, F. H. Zhang, Y. S. Zhu, C. Lu, X. Y. Kuang, J. Lv and P. Shao, *Sci. Rep.*, 2015, **5**, 1–12, DOI: 10.1038/srep15951.
34 The pdb file of the zinc finger protein with accession code 1ZNF was taken and modelled with a chimera software suite (ref. 36).
35 M. A. Franzman and A. M. Barrios, *Inorg. Chem.*, 2008, **47**(10), 3928–3930.
36 E. F. Pettersen, T. D. Goddard, C. C. Huang, G. S. Couch, D. M. Greenblatt, E. C. Meng and T. E. Ferrin, *J. Comput. Chem.*, 2004, **25**(13), 1605–1612.